Article

Thiolactones and $\Delta^{8,9}$-Pregnene Steroids from the Marine-Derived Fungus *Meira* sp. 1210CH-42 and Their *α*-Glucosidase Inhibitory Activity

Hee Jae Shin [1,2,*], Min Ah Lee [1,3], Hwa-Sun Lee [1,3] and Chang-Su Heo [1,2]

1   Marine Natural Products Chemistry Laboratory, Korea Institute of Ocean Science and Technology, 385 Haeyang-ro, Yeongdo-gu, Busan 49111, Republic of Korea; minah@kiost.ac.kr (M.A.L.); hwasunlee@kiost.ac.kr (H.-S.L.); science30@kiost.ac.kr (C.-S.H.)
2   Department of Marine Biotechnology, University of Science and Technology (UST), 217 Gajungro, Yuseong-gu, Daejeon 34113, Republic of Korea
3   Department of Chemistry, Pukyong National University, Busan 48513, Republic of Korea
*   Correspondence: shinhj@kiost.ac.kr; Tel.: +82-51-664-3341; Fax: +82-51-664-3340

Abstract: The fungal genus *Meira* was first reported in 2003 and has mostly been found on land. This is the first report of second metabolites from the marine-derived yeast-like fungus *Meira* sp. One new thiolactone (**1**), along with one revised thiolactone (**2**), two new $\Delta^{8,9}$-steroids (**4**, **5**), and one known $\Delta^{8,9}$-steroid (**3**), were isolated from the *Meira* sp. 1210CH-42. Their structures were elucidated based on the comprehensive spectroscopic data analysis of 1D, 2D NMR, HR-ESIMS, ECD calculations, and the pyridine-induced deshielding effect. The structure of **5** was confirmed by oxidation of **4** to semisynthetic **5**. In the *α*-glucosidase inhibition assay, compounds **2**–**4** showed potent in vitro inhibitory activity with IC_{50} values of 148.4, 279.7, and 86.0 μM, respectively. Compounds **2**–**4** exhibited superior activity as compared to acarbose (IC_{50} = 418.9 μM).

Keywords: marine fungus; natural product; *Meira* sp.; thiolactone; pregnene steroid; epimer; stereochemistry; *α*-glucosidase inhibitor

1. Introduction

Fungi constitute one of the largest groups of organisms. Fungal-derived natural products (NPs) are pharmaceutically abundant, with several important biological applications ranging from highly potent toxins to approved drugs [1]. In particular, secondary metabolites obtained from marine fungi have garnered significant interest due to their unique chemical structures and potential biomedical applications [1,2]. While the number of cultivable marine fungi is extremely low (1% or less) compared to their global biodiversity [1,3], more than 1000 molecules have been reported and characterized from marine fungi, including alkaloids, lipids, peptides, polyketides, prenylated polyketides, and terpenoids [4–7]. Most research on secondary metabolites produced by marine fungi has primarily focused on a few genera, including *Penicillium*, *Aspergillus*, *Fusarium*, and *Cladosporium* [8,9]. Research into natural products derived from marine fungi is continually expanding, and as a result, a broader range of genera is now being investigated, with a particular focus on those associated with unique substrates and previously unexplored habitats [10–12].

In 2003, the genus *Meira* was first reported, namely *M. geulakonigii* and *M. argovae*, as a novel basidiomycetous [13]. *M. geulakonigii* was isolated from the citrus rust mite on pummelo (*Citrus grandis*), and *M. argovae* originated from a carmine spider mite on the leaves of castor bean (*Ricinus communis*) [8]. These *Meira* species have a similar morphology to yeast-like fungi. Nonetheless, the phylogenetic analysis of rDNA sequence data has identified *Meira* as a member of the Brachybasidiaceae family within the Exobasidiales, which

is classified under the Ustilaginomycetes (Basidiomycota) in the Exobasidiomycetidae group [14]. *M. geulakonigii* has been used successfully as a biological control agent against citrus and other phytophagous mites, as well as powdery mildew fungi [13,15–17]. A potential biocontrol agent against five mite species has been demonstrated for *M. argovae* [18]. Recently, *M. nicotianae* came from the rhizosphere of tobacco root, and that strain has the capability to promote plant growth possible in similar ways as plant growth-promoting fungi and arbuscular mycorrhizal fungi [19].

In this study, we isolated a yeast-like fungal species from a seawater sample. Phylogenetic analysis of ITS rDNA indicated that strain 1210CH-42 is closely related to other *Meira* species: *Meira* sp. M40, *M. nashicola* CY-1, and *M. miltonrushii* NIOSN-SK46-S121. So far, there are only a few reports on the isolation of *Meira* strains, but natural products from the genus *Meira* have not been investigated. This is the first report on the secondary metabolites from the marine-derived yeast-like fungus *Meira*. Herein, we report the isolation, structure elucidation, α-glucosidase inhibitory activity of **1–5**, and the structure revision of **2** isolated from the *Meira* strain 1210CH-42 (Figure 1).
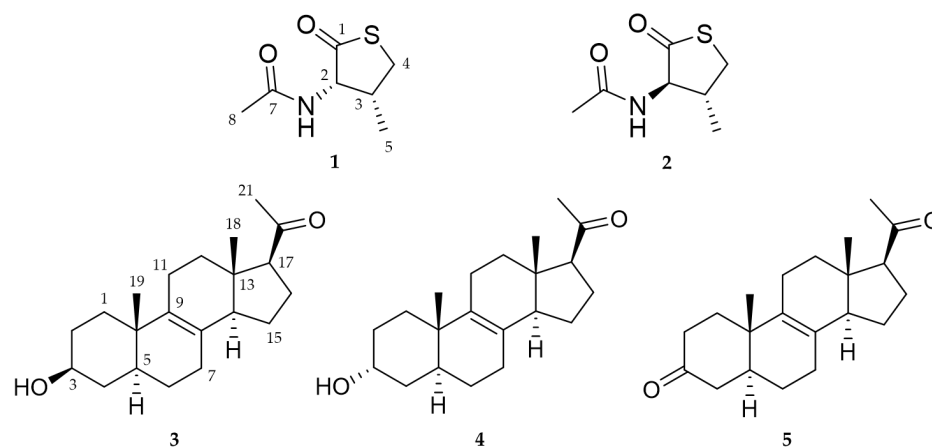
Figure 1. Structures of **1–5** from the marine fungus strain *Meira* sp. 1210CH-42.

2. Results and Discussion

### 2.1. Structure Elucidation of New Compounds

Compound **1** was obtained as a white amorphous powder, and its molecular formula was determined to be $C_7H_{11}NO_2S$ by HR-ESIMS, with three degrees of unsaturation. The ^1H and ^{13}C NMR data of **1** are summarized in Table 1. The ^1H NMR spectrum of **1** in CD_3OD revealed two methine protons (δ_H 4.79 and 2.86), one methylene proton (δ_H 3.64 and 3.10), and two methyl protons (δ_H 2.03 and 1.04). The ^{13}C NMR and HSQC spectra showed the presence of seven signals, including two carbonyl carbons (δ_C 206.5 and 173.8), two methines (δ_C 63.9 and 36.0), one methylene (δ_C 35.9) and two methyl carbons (δ_C 22.4 and 13.0). The planar structure of **1** was elucidated by analysis of ^1H-^1H COSY and HMBC correlations (Figure 2). The COSY correlations from H-2 (δ_H 4.79)/H-3 (δ_H 2.86), H-3 (δ_H 2.86)/H-4 (δ_H 3.64), and H-3 (δ_H 2.86)/H-5 (δ_H 1.04) were observed. In addition, the HMBC correlations from H-2 (δ_H 4.79) to C-1 (δ_C 206.5)/C-3 (δ_C 36.0)/C-5 (δ_C 13.0)/C-7 (δ_C 173.8), H-4 (δ_H 3.10 and 3.64) to C-1 (δ_C 206.5)/C-2 (δ_C 63.9)/C-5 (δ_C 13.0) and H-8 (δ_H 2.03) to C-7 (δ_C 206.5) suggested that **1** has a ring system, and confirmed the planar structure of **1**.

Detailed analysis of $^3J_{H,H}$ coupling constants and 1D NOESY data determined the relative configuration of **1**. The relative stereochemistry of C-2 could be established by the observation of strong selective 1D NOESY correlations between H-2 and H-3/H-4b, between H-4b and H-2/H-3, and between H-5 and H-4a (Figure 2). These correlations suggested that the relative configurations of C-2 and C-3 must be *cis* rather than *trans*-configuration in **1**. Thus, the relative configuration of **1** could be assigned as 2*S**, 3*R**. To determine the absolute configuration of **1**, the theoretical electronic circular dichroism (ECD) spectra of **1** and its enantiomer were calculated. The experimental ECD spectrum of **1**

showed a good agreement with the calculated ECD spectrum of the 2*S*, 3*R*-isomer (Figure 3). Therefore, the structure of **1** was elucidated to be a 2*S*-acetamide-3*R*-methyl-thiolactone.

Table 1. ^{1}H and ^{13}C NMR data of **1** and **2** (600 MHz for ^{1}H and 150 MHz for ^{13}C, in CD$_3$OD).

Position	1		2	
	δ_C, Type	δ_H, Mult. (*J* in Hz)	δ_C, Type	δ_H, Mult. (*J* in Hz)
1	206.5, C		206.5, C	
2	63.9, CH	4.79, d (6.6)	65.7, CH	4.29, d (12.5)
3	36.0, CH	2.86, m	40.2, CH	2.37, m
4a	35.9, CH$_2$	3.10, dd (11.4, 2.2)	34.7, CH$_2$	3.08, t (11.2)
4b		3.64, dd (11.4, 5.4)		3.34, d (11.2)
5	13.0, CH$_3$	1.04, d (6.9)	17.5, CH$_3$	1.20, d (6.5)
6-NH				
7	173.8, C		174.0, C	
8	22.4, CH$_3$	2.03, s	22.6, CH$_3$	2.02, s
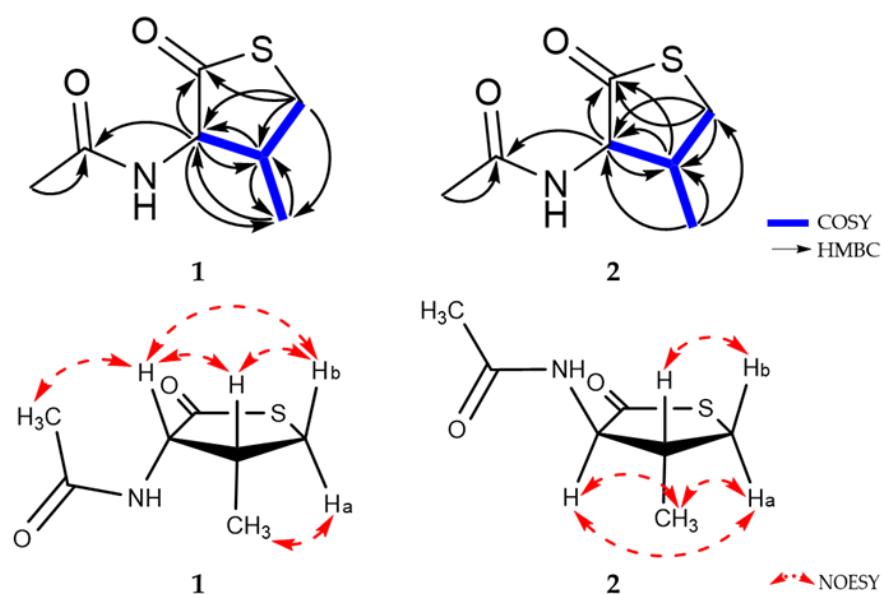
Figure 2. ^{1}H-^{1}H COSY and key 2D NMR correlations of **1** and **2**.
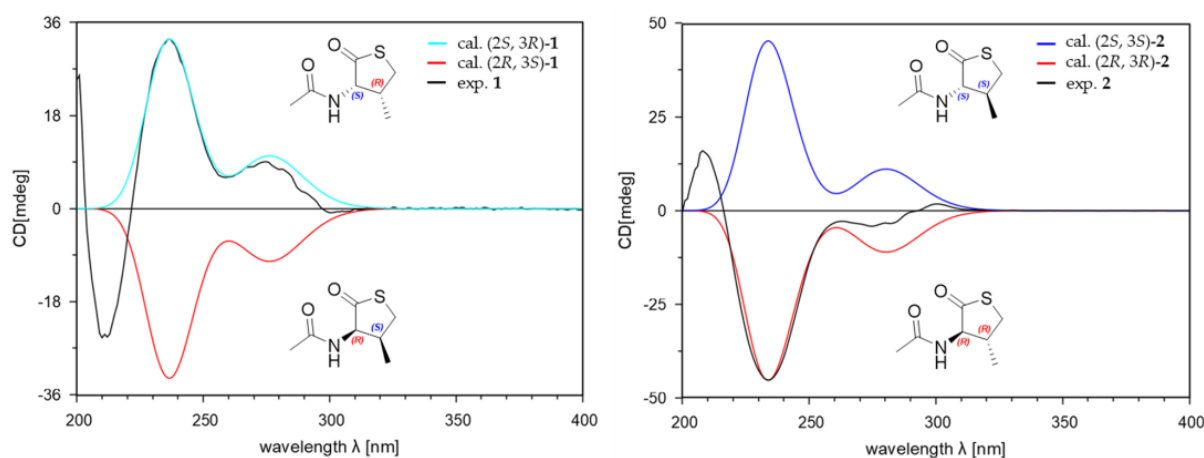
Figure 3. Experimental CD spectra and the calculated ECD spectra of **1** and **2**.

Compound **2** was isolated as a white amorphous powder. The molecular formula of **2** was the same as that of **1** (C$_7$H$_{11}$NO$_2$S) based on the HR-ESIMS data. Furthermore,

the 1D NMR data of **2** were also similar but not identical to those of **1** (Table 1). The planar structure of **2** was determined to be the same as **1** by analysis of ^{1}H-^{1}H COSY and HMBC data (Figure 2). However, the ^{1}H and ^{13}C chemical shifts of **2** were different from **1**, especially those for the chiral centers, suggesting that the stereochemistry of **2** might be different from **1**. The relative configuration of **2** was also determined by analysis of $^3J_{H,H}$ coupling constants and selective 1D NOESY data. The relative stereochemistry of C-2 could be established through the observation of strong NOESY contacts between H-2 and H-4a/H-5, between H-4a and H-2/H-5, and between H-4b and H-3. A relatively large coupling constant was observed between H-2 and H-3 ($^3J_{H,H}$ = 12.5 Hz). Thus, the relative configurations of H-2 and H-3 had a *trans*-configuration in **2** (Figure 2). The *J*-based configurational analysis and NOESY measurements could not discriminate the possible relative configurations for (2*S**, 3*S**) or (2*R**, 3*R**). To solve this issue and to determine the absolute configuration of **2**, the ECD spectra of **2** and its enantiomer were calculated. The experimental ECD spectrum of **2** showed a good agreement with the calculated ECD spectrum of the 2*R*, 3*R*-isomer (Figure 3). Therefore, the structure of **2** was elucidated as an epimer of **1** and to be a 2*R*-acetamide-3*R*-methyl-thiolactone.

Notably, the ^{1}H and ^{13}C NMR data in CDCl$_3$ of **2** were almost the same as those of the previously reported thiolactone with 2*R*, 3*S*-configuration isolated from a *Penicillium chrysogenum* (Table S1 and Figure S15) [20]. The reported compound with 2*R*, 3*S*-configuration possesses the same planar structure as **2** in this study. In the original paper for the compound with 2*R*, 3*S*-configuration, by the NOE correlation between H-3 (δ_H 2.24) and H-2 (δ_H 4.45), the authors insisted that the two protons were oriented on the same side of the ring system. However, its 1D NOE spectrum for the reported compound showed signals from H-3 (δ_H 2.24) to H-2/H-4/H-5/H-6 and NH, making it unclear to determine the orientation of H-3 to the same side of H-2 or not (Figures S15 and S16). Moreover, if the reported configuration is correct, H-2 and H-3 are in *syn* relation, and they should have a small scalar coupling constant, but H-2 in the reported thiolactone had a large coupling constant (12.5 Hz) as in the revised structure (Table S1). In this study, we carefully compared and checked the selective 1D NOESY data of **2** with those for the reported compound. As noted above, **2** exhibited strong NOE correlations from H-2 to H-5/H-4a and from H-4b to H-3 but not from H-4b to H-2, suggesting that H-2 and H-5 are on the same face. Furthermore, the reported compound with 2*R*, 3*S*-configuration and **1** (2*S*, 3*R*-configuration) are enantiomers and should have the same but opposite-in-sign specific rotation values. However, the optical rotation values of the reported thiolactone and **1** were $[\alpha]_D^{25}$ +1.5 (*c* 0.1, MeOH) and $[\alpha]_D^{25}$ +60.0 (*c* 0.1, MeOH), respectively. Considering all these results, the structure of the reported compound (2*R*, 3*S*-configuration) should be revised to 2*R*-acetamide-3*R*-methyl-thiolactone (Figure 4).
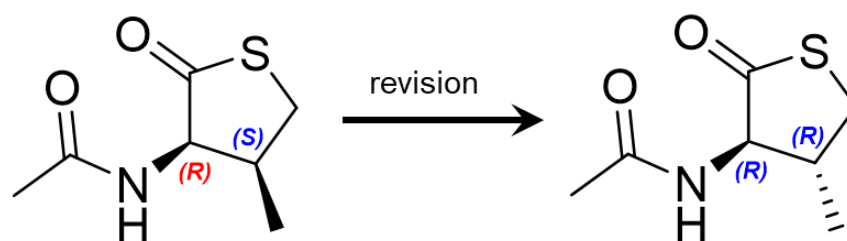

Figure 4. Reported and revised structures of **2**.

Compound **3** was isolated as a white amorphous powder, and its molecular formula was determined to be C$_{21}$H$_{32}$O$_2$. By the comparison of the ^{1}H and ^{13}C NMR (Table 2), HR-ESIMS, and optical rotation data of **3** with those reported previously in the literature, **3** was identified as a known compound, (+)-03219A, $\Delta^{8,9}$-3β-hydroxy-5α-17-acetyl steroid [21–23].

Table 2. ^{1}H and ^{13}C NMR data of **3–5** (600 MHz for ^{1}H and 150 MHz for ^{13}C, in CD$_3$OD).

| Position	3		4		5	
	δ_C, Type	δ_H, Mult. (*J* in Hz)	δ_C, Type	δ_H, Mult. (*J* in Hz)	δ_C, Type	δ_H, Mult. (*J* in Hz)
1a	36.6, CH$_2$	1.22, td (16.2, 5.2)	32.0, CH$_2$	1.55, m	38.0, CH$_2$	1.55, m
1b		1.80, o.l [1]				
2a	32.4, CH$_2$	1.42, o.l	37.1, CH$_2$	1.48, o.l	39.1, CH$_2$	2.31, o.l
2b		1.80, o.l		1.54, o.l		2.53, m
3	71.8, CH	3.53, m	67.2, CH	3.97, t (2.8)	214.6, C	
4a	39.2, CH$_2$	1.31, o.l	30.0, CH$_2$	1.68, m	45.7, CH$_2$	2.11, o.l
4b		1.61, m				2.40, t (14.6)
5	42.3, CH	1.40, o.l	36.4, CH	1.86, m	44.4, CH	1.80, m
6a	26.8, CH$_2$	1.39, o.l	26.7, CH$_2$	1.32, m	26.7, CH$_2$	1.47, o.l
6b		1.52, m		1.46, o.l		1.60, m
7	28.5, CH$_2$	2.02, m	28.4, CH$_2$	2.02, m	28.4, CH$_2$	2.04, m
8	129.2, C		129.0, C		130.1, C	
9	136.3, C		137.2, C		135.6, C	
10	37.1, CH		37.6, CH		37.3, CH	
11a	24.0, CH$_2$	2.15, m	23.6, CH$_2$	2.13, o.l	24.1, CH$_2$	2.20, m
11b		2.27, o.l		2.28, o.l		2.25, o.l
12a	37.3, CH$_2$	1.69, m	37.3, CH$_2$	1.70, o.l	37.2, CH$_2$	1.70, o.l
12b		2.07, m		2.07, o.l		2.08, o.l
13	45.0, C		45.1, C		45.0, C	
14	53.3, CH	2.27, o.l	53.4, CH	2.30, o.l	53.2, CH	2.29, m
15a	25.3, CH$_2$	1.42, o.l	25.3, CH$_2$	1.42, o.l	25.3, CH$_2$	1.45, o.l
15b		1.72, m		1.72, o.l		1.72, o.l
16a	24.3, CH$_2$	1.72, o.l	24.2, CH$_2$	1.72, o.l	24.3, CH$_2$	1.72, o.l
16b		2.21, m		2.21, m		2.21, m
17	63.5, CH	2.69, t (8.7)	63.5, CH	2.70, t (8.6)	63.5, CH	2.70, t (8.7)
18	13.2, CH$_3$	0.57, s	13.2, CH$_3$	0.57, s	13.2, CH$_3$	0.60, s
19	18.3, CH$_3$	0.97, s	17.3, CH$_3$	0.94, s	17.3, CH$_3$	1.18, s
20	212.4, C		212.5, C		212.3, C	
21	31.7, CH$_3$	2.13, s	31.7, CH$_3$	2.13, s	31.7, CH$_3$	2.14, s

[1] Signals were overlapped with other signals.

Compound **4** was purified as a white amorphous powder, and its molecular formula was determined to be C$_{21}$H$_{32}$O$_2$ by HR-ESIMS, which is identical to that of **3**, with 6 degrees of unsaturation. The ^{1}H and ^{13}C NMR data of **4** are summarized in Table 2. The ^{1}H NMR data for **4** revealed the signals of three methyl groups (δ_H 0.57, 0.94, and 2.13), one oxymethine (δ_H 3.97), nine methylenes, and three sp^3 methines. The ^{13}C NMR and HSQC data of **4** exhibited 21 carbon signals containing three methyls (δ_C 13.2, 17.3, and 31.7), one oxymethine (δ_C 67.2), nine methylenes, two olefinic quaternary carbons (δ_C 129.0 and 137.2), two sp^3 quarternary carbons (δ_C 37.6 and 45.1), and one ketone carbonyl carbon (δ_C 212.5). The planar structure of **4** was elucidated by ^{1}H-^{1}H COSY and HMBC data (Figure 5). The ^{1}H-^{1}H COSY correlations suggested the presence of four ^{1}H-^{1}H spin systems: from H-1 to H-4, from H-5 to H-7, from H-11 to H-12, and from H-14 to H-17. The HMBC correlations from H-6/H-7/H-11/H-14/H-15 to C-8 (δ_C 129.0) and from H-11/H-12/H-14/H-19 to C-9 (δ_C 137.2) indicated a double bond was located at C-8 and C-9. Additionally, the HMBC correlations from H-21 to C-17 (δ_C 63.5)/C-20 (δ_C 212.5) supported the assignment of an acetyl moiety connected to C-17 of the five-membered ring. The planar structure of **4** was the same as that of **3**, (+)-03219A [23], except for the difference in the chemical shifts around the oxymethine (δ_H 3.97 and δ_C 67.2) at C-3, suggesting that the stereochemistry of C-3 might be different from **3** (Figure 1 and Table 2). The stereochemistry of **4** was determined by analysis of the ROESY spectrum, 1D NOESY data, coupling constants, and the pyridine-induced deshielding effect. The relative configuration of **4** was confirmed by the ROESY correlations from H-3 to H-2a/H-2b/H-4, from H-19 to H-2b/H-4/H-11/H-18, and from H-18 to H-15/H-21 (Figure 5). The selective 1D NOE correlations were observed

from H-3 to H-2a/H-2b/H-4/H-19 (Figure S27). Furthermore, the small coupling constant of H-3 at δ_H 3.97 (t, J = 2.8) was indicative of the C-3 hydroxyl group being axial from an examination of the Dreiding model (Table 2 and Figure 5) [24]. The significant deshielded chemical shifts of H$_{eq}$-3 ($\Delta\delta_H$ = +0.32) and H$_{ax}$-5 ($\Delta\delta_H$ = +0.48) in pyridine-d_5 compared with those in CD$_3$OD indicated that OH-3 and H-5 adopted α-orientation, supporting the identified orientation (Figure 6 and Figure S29) [25–28]. Consequently, the structure of **4** was determined as a new epimer of **3**, $\Delta^{8,9}$-3α-hydroxy-5α-17-acetyl steroid.
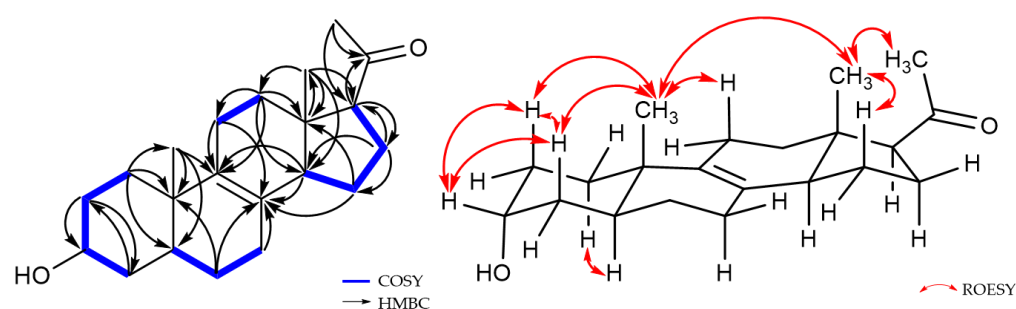
Figure 5. ^{1}H-^{1}H COSY and key 2D NMR correlations of **4**.
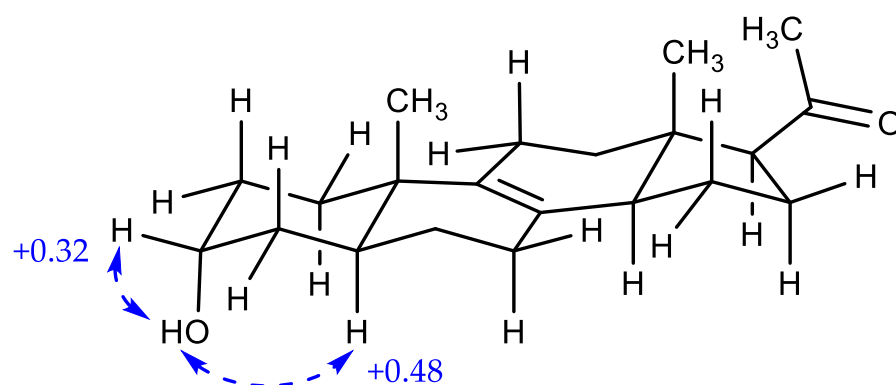
Figure 6. Pyridine-induced deshielding effects of **4** ($\Delta\delta$ = δ_H in C$_5$D$_5$N-δ_H in CD$_3$OD).

Compound **5** was obtained as a white amorphous powder. The NMR data of **5** were similar to those of **4**, except for the absence of signals for the oxymethine at C-3 (δ_H 3.97 and δ_C 67.2) in **4** and the appearance of a ketone signal at C-3 (δ_C 214.6) in **5** (Table 2), revealing that **5** would be an oxidized form of **4**. The ^{1}H and ^{13}C NMR spectra, compared to those of **3** and **4**, showed the significantly deshielded chemical shifts of C-2 (δ_H 2.31/2.53 and δ_C 39.1) and C-4 (δ_H 2.11/2.40 and δ_C 45.7). Additionally, the HMBC correlations between H-2b (δ_H 2.53)/H-4 (δ_H 2.11/2.40) and C-3 (δ_C 214.6) determined the position of the ketone at C-3 (Figure 7). To clearly confirm the structure of **5**, **4** was oxidized to obtain the semisynthetic **5**. Both **5** and semisynthetic **5** exhibited identical ^{1}H NMR, HSQC, and HMBC spectra (Figures S35, S36 and S37). The molecular formula of semisynthetic **5** was determined to be C$_{21}$H$_{30}$O$_2$ by HR-ESIMS (m/z 337.2134 [M + Na]$^+$, calcd. for C$_{21}$H$_{30}$O$_2$Na, 337.2138). Based on these results, the structure of **5** was determined as a 3-keto derivative of **4**, with 7 degrees of unsaturation. Therefore, the structures of **5** and semisynthetic **5** were designated as $\Delta^{8,9}$-5α-3,20-dione-17-acetyl steroids.

2.2. α-Glucosidase Inhibitory Activities of Compounds

Compounds **1**–**4** were evaluated for α-glucosidase inhibitory activities (Table 3). Compound **4** exhibited the most significant inhibitory effect with an IC$_{50}$ value of 86.0 μM, while **2** and **3** showed moderate activities with IC$_{50}$ values of 148.4 and 279.7 μM, respectively. Further, **1** exhibited weak inhibitory activity at a concentration of 400 μM. The change in the stereochemistry of the compounds remarkably altered the α-glucosidase inhibitory

activities. Compounds **1** and **2**, as well as **3** and **4**, are stereoisomers of each other. Compounds **2** and **4** showed stronger α-glucosidase inhibitory effects than **1** and **3**. It could be noted herein that the stereochemistry was important for α-glucosidase inhibitory activity.
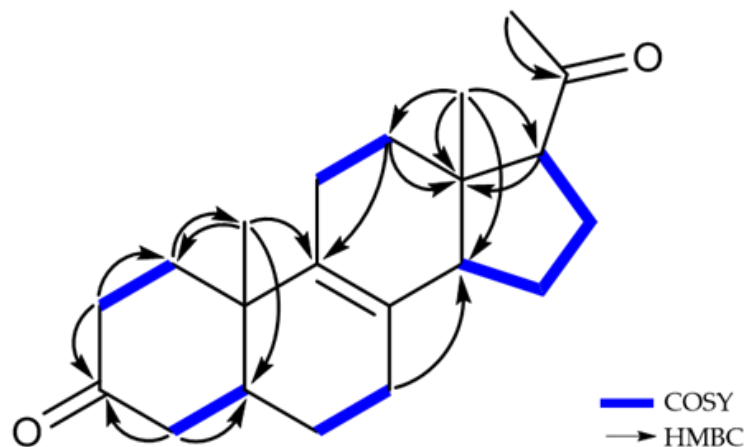

Figure 7. ^{1}H-^{1}H COSY and key HMBC correlations of **5**.

Table 3. α-Glucosidase inhibitory activities of **1**–**4**.

Compounds	IC$_{50}$ (μM) [1]
1	>400
2	148.4
3	279.7
4	86.0
Acarbose [2]	418.9

[1] The 50% inhibitory concentration (μM). [2] Acarbose is used as a positive control.

3. Materials and Methods

3.1. General Experimental Procedures and Reagents

NMR spectra were acquired with a Bruker AVANCE III 600 spectrometer (Bruker BioSpin GmbH, Rheinstetten, Germany) with a 3 mm probe operating at 600 MHz (^{1}H) and 150 MHz (^{13}C). Chemical shifts were expressed in ppm with reference to the solvent peaks (δ_H 3.31 and δ_C 49.15 ppm for CD$_3$OD, δ_H 7.26 and δ_C 77.26 ppm for CDCl$_3$). UV spectra were recorded with a Shimadzu UV-1650PC spectrophotometer (Shimadzu Corporation, Kyoto, Japan). IR spectra were obtained on a JASCO FT/IR-4100 spectrophotometer (JASCO Corporation, Tokyo, Japan). Optical rotations were measured with a Rudolph analytical Autopol III S2 polarimeter (Rudolph Research Analytical, Hackettstown, NJ, USA). LR-ESIMS data were obtained with an ISQ EM mass spectrometer (Thermo Fisher Scientific Korea Ltd., Seoul, Republic of Korea). HR-ESIMS data were obtained with a Waters SYNPT G2 Q-TOF mass spectrometer (Waters Corporation, Milford, CT, USA) at Korea Basic Science Institute (KBSI) in Cheongju, Republic of Korea and a Sciex X500R Q-TOF spectrometer (Framingham, MA, USA). ECD spectra were recorded with a JASCO J-1500 polarimeter at the Center for Research Facilities, Changwon National University, Changwon, Republic of Korea. HPLC was performed using a BLS-Class pump (Teledyne SSI, Inc., State College, PA 16803, USA) with Shodex RI-201H refractive index detector (Shoko Scientific Co., Ltd., Yokohama, Japan). Columns for HPLC were YMC-ODS-A (250 mm $\times$ 10 mm, 5 μm; and 250 mm $\times$ 10 mm, 5 μm) and YMC-Triart (250 mm $\times$ 10 mm, 5 μm; and 250 mm $\times$ 10 mm 5 μm). C$_{18}$-reversed-phase silica gel (YMC-Gel ODS-A, 12 nm, S-75 μm) was used for open-column chromatography. Organic solvents were purchased as HPLC grade, and ultrapure waters were obtained from the Milipore Mili-Q Direct 8 system (Milipore S.A.S. Molsheim, France). The reagents used in the bioassay were purchased

from Sigma-Aldrich (Merck Korea, Seoul, Republic of Korea) and Tokyo Chemical Industry (TCI Co., Ltd., Tokyo, Japan).

3.2. Fungal Strain and Fermentation

The strain 1210CH-42 was isolated from a seawater sample collected at Chuuk Islands, Federated States of Micronesia, in 2010. The seawater sample was filtered, concentrated, and diluted (10^{-1} and 10^{-2}) with sterile seawater under aseptic conditions. Then the diluted sample was spread on Bennett's agar plates (1% D-glucose, 0.2% tryptone, 0.1% yeast extract, 0.1% beef extract, 0.5% glycerol, 1.7% agar, sea salt 32 g/L, pH 7.0). The plates were incubated for 7 days at 28 °C, and the single colony of the strain 1210CH-42 was collected. The fungus was identified as *Meira* sp. (GenBank accession number OQ693946) by DNA amplification and sequencing of the ITS region of the rRNA gene. The used primers were ITS4 (TCCTCCGCTTATTGATATGC) and ITS5 (GGAAGTAAAAGTCGTAACAAG G). The cultures of the strain 1210CH-42 were performed in modified Bennett's broth medium (1% D-glucose, 0.2% tryptone, 0.1% yeast extract, 0.1% beef extract, 0.5% glycerol, sea salt 10 g/L, pH 7.0). A seed culture was prepared from a spore suspension of the strain 1210CH-42 by inoculating into 1 L flasks and incubating it at 28 °C for 5 days on a rotary shaker at 120 rpm. The seed culture was inoculated aseptically into 2 L flasks (total 32 flasks) containing 1.0 L of medium and a 20 L fermenter containing 18 L of sterilized culture medium (0.1% *v/v*), respectively. The large-scale fermentation was done under the same conditions as the seed culture for 8 days and then harvested.

3.3. Extraction and Isolation of Compounds **1**–**5**

The culture broth (total 50 L) of the strain 1210CH-42 was harvested by high-speed centrifugation (60,000 rpm), and then the supernatant was extracted two times with ethyl acetate (100 L). The EtOAc extract was evaporated to afford a crude extract (3.05 g). The crude extract was subjected to ODS open column chromatography (YMC Gel ODS-A, 12 nm, S75 μm) followed by stepwise gradient elution with MeOH/H_2O (*v/v*) (20:80, 40:60, 60:40, 80:20, and 100:0) as eluent. The 20% MeOH fraction was purified by a reversed-phase HPLC (YMC ODS-A column, 250 × 10 mm i.d., 5 μm; 10% MeOH in H_2O; flow rate: 1.5 mL/min; detector: RI) to yield **1** (2.9 mg, t_R 44.0 min). Peak 10 from the 20% MeOH fraction was further purified by a reversed-phase HPLC (YMC ODS-A column, 250 × 10 mm i.d., 5 μm; 5% MeOH in H_2O; flow rate: 1.5 mL/min; detector: RI) to yield **2** (0.6 mg, t_R 64.0 min). The 80% MeOH fraction was purified by a reversed-phase HPLC (YMC ODS-A column, 250 × 10 mm i.d., 5 μm; 70% MeOH in H_2O; flow rate: 1.5 mL/min; detector: RI) to yield **3** (0.6 mg, t_R 84.0 min), **4** (2.1 mg, t_R 95.5 min), and **5** (0.3 mg, t_R 79.0 min).

Compound **1**: White amorphous powder; $[\alpha]_D^{25}$ +60.0 (*c* 0.1, MeOH); UV (MeOH) λ_{max} (log ε) 204 (3.64), 235 (3.33) nm; IR (MeOH) ν_{max} 3296, 2940, 1667, 1548, 1448, 1021 cm^{-1}; ^{1}H and ^{13}C NMR data (CD$_3$OD), see Table 1; HR-ESIMS *m/z* 196.0408 [M + Na]$^+$, calcd. for C$_7$H$_{11}$NO$_2$NaS, 196.0408.

Compound **2**: White amorphous powder; $[\alpha]_D^{25}$ +10.0 (*c* 0.1, MeOH); UV (MeOH) λ_{max} (log ε) 206 (3.88), 234 (3.69) nm; IR (MeOH) ν_{max} 3275, 2933, 1700, 1650, 1548, 1448, 1021 cm^{-1}; ^{1}H and ^{13}C NMR data (CD$_3$OD), see Table 1; HR-ESIMS *m/z* 196.0406 [M + Na]$^+$, calcd. for C$_7$H$_{11}$NO$_2$NaS, 196.0408.

Compound **3**: White crystalline needles; $[\alpha]_D^{25}$ +86.0 (*c* 0.1, MeOH); UV (MeOH) λ_{max} (log ε) 202 (4.10) nm; IR (MeOH) ν_{max} 3371, 2925, 2855, 1703, 1452, 1357, 1032 cm^{-1}; ^{1}H and ^{13}C NMR data (CD$_3$OD), see Table 2; HR-ESIMS *m/z* 339.2297 [M + Na]$^+$, calcd. for C$_{21}$H$_{32}$O$_2$Na, 339.2300.

Compound **4**: White crystalline needles; $[\alpha]_D^{25}$ +97.3 (*c* 0.1, MeOH); UV (MeOH) λ_{max} (log ε) 202 (3.96) nm; IR (MeOH) ν_{max} 3286, 2925, 2870, 1703, 1452, 1353, 1025 cm^{-1}; ^{1}H and ^{13}C NMR data (CD$_3$OD), see Table 2; HR-ESIMS *m/z* 339.2301 [M + Na]$^+$, calcd. for C$_{21}$H$_{32}$O$_2$Na, 339.2300.

Compound **5**: White amorphous; $[\alpha]_D^{25}$ +63.3 (*c* 0.1, MeOH); UV (MeOH) λ_{max} (log ε) 204 (3.86) nm; IR (MeOH) ν_{max} 3378, 2933, 2866, 1707, 1456, 1367, 1036 cm^{-1}; ^{1}H and ^{13}C NMR data (CD$_3$OD), see Table 2.

Oxidation of **4**. To a compound **4** (2.0 mg, 6.32 μmol) in anhydrous CH$_2$Cl$_2$ (0.5 mL) was added Dess-Martin reagent (8.04 mg, 18.96 μmol) at 0 °C. The mixture was stirred at r.t. for 24 h under N$_2$ gas. The solution was washed with 5% NaHCO$_3$ and brine and concentrated under reduced pressure [29,30]. Then the reactant was partitioned with EtOAc and H$_2$O. The EtOAc layer was concentrated, and subjected to a reversed-phase HPLC (YMC-Triart C$_{18}$ column, 250 × 10 mm i.d., 5 μm; 70% MeOH in H$_2$O; flow rate: 2.0 mL/min; detector: RI) to yield semisynthetic **5** (0.5 mg): white amorphous solid; ^{1}H NMR (600 MHz, CD$_3$OD, representative signals) δ_H 2.71 (t, *J* = 8.7 Hz, 1H), 2.53–2.31 (m, 2H), 2.40–2.08 (t, *J* = 14.6, o. l, 2H), 2.30 (o. l, H), 2.23 (o. l, 2H), 2.14 (s, 3H), 2.21–1.71 (o. l, 2H), 2.07 (o. l, 2H), 1.81 (m, 2H), 1.70–1.47 (o. l, 2H), 1.56 (o. l, 2H), 1.45 (o. l, 2H), 1.18 (s, 3H), 0.60 (s, 3H); ^{13}C NMR data from HMBC spectrum (CD$_3$OD, representative signals) δ_C 214.5, 212.3, 135.6, 130.4, 63.5, 53.2, 45.7, 45.0, 44.4, 39.1, 38.1, 37.2, 31.7, 28.4, 26.7, 25.3, 24.3, 24.1, 23.7, 17.5, 13.1; HR-ESIMS *m/z* 327.2134 [M + Na]$^+$, calcd. for C$_{21}$H$_{30}$O$_2$Na, 327.2138.

3.4. Computational Analysis

The initial geometry optimization and conformational searches were generated using the Conflex 8 (Rev. B, Conflex Corp., Tokyo, Japan). The optimization and calculation for ECD were carried out using the Gaussian 16 program (rev. B.01, Gaussian Corp., Wallingford, C.T., USA). Conformational searches were performed using MMFF94s force field calculations with a 10 kcal/mol search limit. The conformers were optimized using the ground state method at the B3LYP/6-311+G (d, p) level in MeOH with a default model for ECD. The theoretical calculations of ECD spectra were performed using TD-SCF at the B3LYP /6-311+G (d, p) level in the gas phase. The ECD spectra were simulated by SpecDis (v. 1.71) using σ = 0.30–0.50 eV. All calculated curves were shifted to +10 nm to simulate experimental spectra better.

3.5. Measurement of α-Glucosidase Inhibitory Activity

The evaluation of α-glucosidase inhibitory activity was performed with reference to previously reported literature [31,32]. All the assays were carried out under 0.1 M PBS buffer (pH 7.4, Sigma). The samples (10 mM) were dissolved with DMSO (Sigma) and diluted into gradient concentrations with PBS buffer. The pre-reaction mixture consisted of the 130 μL sample with 30 μL α-glucosidase solution (0.2 U/mL, Sigma) and shaken well, then added to a 96-well plate and placed at 37 °C for 10 min in an incubator. Subsequently, 40 μL of 5 mM *p*-nitrophenyl-α-D-glucopyranoside (*p*NPG, TCI) was added and further incubated at 37 °C for 20 min. Finally, the α-glucosidase inhibitory activity was determined by measuring the release of *p*NPG at 405 nm of the microplate reader. The negative control was prepared by adding PBS buffer instead of the sample in the same way as the test. The blank was prepared by adding PBS buffer instead of *p*NPG using the same method. Acarbose was used as the positive control, and experiments were carried out in triplicate.

4. Conclusions

In summary, one new thiolactone (**1**), along with one revised thiolactone (**2**), two new $\Delta^{8,9}$-steroids (**4, 5**), and one known $\Delta^{8,9}$-steroid (**3**), were isolated from the marine-derived fungus *Meira* sp. 1210CH-42. The absolute configurations of **1** and **2** were determined by analysis of the selective 1D NOESY and ECD data. Compounds **1** and **2** were identified as a pair of acetamide epimers at C-2. While compounds **3** and **4** were identified as epimers for the hydroxyl group at C-3, which was confirmed by analysis of ^{1}H NMR, ROESY, 1D NOESY, coupling constants, and the pyridine-induced deshielding effect. In addition, the structure of **5** was obtained as the 3-keto derivative of **3**. Compounds **1–4** were screened for their α-glucosidase inhibitory activity preliminarily. Compound **4** exhibited intense activity with an IC$_{50}$ value of 86.0 μM. Furthermore, compounds **2** (IC$_{50}$ = 148.4 μM)

and **3** (IC_{50} = 279.7 μM) demonstrated superior activity as compared to acarbose (IC_{50} = 418.9 μM). To the best of our knowledge, this is the first report of new bioactive metabolites with potent *α*-glucosidase inhibitory activity from the yeast-like fungus *Meira*. These results show that *Meira* sp. 1210CH-42 produces unique and diverse metabolites which have the potential for an anti-diabetic agent. The genus *Meira* is mostly found on land, and secondary metabolites from the marine-derived genus have not yet been reported. Therefore, further research is needed for the marine-derived fungus *Meira* sp. 1210CH-42 to discover novel secondary metabolites and investigate their biological properties.

Supplementary Materials: The following are available online at: https://www.mdpi.com/article/10.3390/md21040246/s1, Figures S1–S14: ^{1}H, ^{13}C NMR, HSQC, COSY, HMBC, selective 1D NOESY, and HR-ESIMS data of **1** and **2**, Table S1 and Figures S15–S16: ^{1}H, ^{13}C NMR data, and 1D NOESY data of the reported compound, Figures S17–S20: ^{1}H, ^{13}C NMR, HSQC, and HR-ESIMS data of **3**, Figures S21–S28: ^{1}H, ^{13}C NMR, HSQC, COSY, HMBC, ROESY, 1D NOESY, and HR-ESIMS data of **4**, Figure S29: Comparison of ^{1}H data of **4** in pyridine-d_5 and in CD$_3$OD, Figures S30–S34: ^{1}H, ^{13}C NMR, HSQC, COSY, and HMBC data of **5**, Figures S35–S38: ^{1}H MMR, HSQC, HMBC, and HR-ESIMS data of semisynthetic **5**.

Author Contributions: Conceptualization, H.J.S.; investigation, M.A.L., H.-S.L. and C.-S.H.; resources, M.A.L.; writing—original draft preparation, M.A.L.; writing—review and editing, H.J.S.; project administration, H.J.S.; funding acquisition, H.J.S. All authors have read and agreed to the published version of the manuscript.

Institutional Review Board Statement: Not applicable.

Data Availability Statement: The data presented in the article are available in the Supplementary Materials.

Conflicts of Interest: The authors declare no conflict of interest.

References

1. Schueffler, A.; Anke, T. Fungal natural products in research and development. *Nat. Prod. Rep.* **2014**, *31*, 1425–1448. [CrossRef] [PubMed]
2. Duraes, F.; Szemeredi, N.; Kumla, D.; Pinto, M.; Kijjoa, A.; Spengler, G.; Sousa, E. Metabolites from Marine-Derived Fungi as Potential Antimicrobial Adjuvants. *Mar. Drugs* **2021**, *19*, 475. [CrossRef] [PubMed]
3. Arrieche, D.; Cabrera-Pardo, J.R.; San-Martin, A.; Carrasco, H.; Taborga, L. Natural Products from Chilean and Antarctic Marine Fungi and Their Biomedical Relevance. *Mar. Drugs* **2023**, *21*, 98. [CrossRef] [PubMed]
4. El-Demerdash, A.; Kumla, D.; Kijjoa, A. Chemical Diversity and Biological Activities of Meroterpenoids from Marine Derived-Fungi: A Comprehensive Update. *Mar. Drugs* **2020**, *18*, 317. [CrossRef]
5. Hafez Ghoran, S.; Kijjoa, A. Marine-Derived Compounds with Anti-Alzheimer's Disease Activities. *Mar. Drugs* **2021**, *19*, 410. [CrossRef]
6. Jiang, M.; Wu, Z.; Guo, H.; Liu, L.; Chen, S. A Review of Terpenes from Marine-Derived Fungi: 2015–2019. *Mar. Drugs* **2020**, *18*, 321. [CrossRef] [PubMed]
7. Rateb, M.E.; Ebel, R. Secondary metabolites of fungi from marine habitats. *Nat. Prod. Rep.* **2011**, *28*, 290–344. [CrossRef]
8. Imhoff, J.F. Natural Products from Marine Fungi-Still an Underrepresented Resource. *Mar. Drugs* **2016**, *14*, 19. [CrossRef]
9. Shin, H.J. Natural Products from Marine Fungi. *Mar. Drugs* **2020**, *18*, 230. [CrossRef]
10. El-Bondkly, E.A.M.; El-Bondkly, A.A.M.; El-Bondkly, A.A.M. Marine endophytic fungal metabolites: A whole new world of pharmaceutical therapy exploration. *Heliyon* **2021**, *7*, e06362. [CrossRef] [PubMed]
11. Gonçalves, M.F.M.; Esteves, A.C.; Alves, A. Marine Fungi: Opportunities and Challenges. *Encyclopedia* **2022**, *2*, 559–577. [CrossRef]
12. Julianti, E.; Abrian, I.A.; Wibowo, M.S.; Azhari, M.; Tsurayya, N.; Izzati, F.; Juanssilfero, A.B.; Bayu, A.; Rahmawati, S.I.; Putra, M.Y. Secondary Metabolites from Marine-Derived Fungi and Actinobacteria as Potential Sources of Novel Colorectal Cancer Drugs. *Mar. Drugs* **2022**, *20*, 67. [CrossRef]

13. Boekhout, T.; Theelen, B.; Houbraken, J.; Robert, V.; Scorzetti, G.; Gafni, A.; Gerson, U.; Sztejnberg, A. Novel anamorphic mite-associated fungi belonging to the Ustilaginomycetes: *Meira geulakonigii* gen. nov., sp nov., *Meira argovae* sp nov and *Acaromyces ingoldii* gen. nov., sp nov. *Int. J. Syst. Evol. Micr.* **2003**, *53*, 1655–1664. [CrossRef] [PubMed]

14. Rush, T.A.; Aime, M.C. The genus *Meira*: Phylogenetic placement and description of a new species. *Anton. Leeuw. Int. J. G.* **2013**, *103*, 1097–1106. [CrossRef]

15. Gerson, U.; Gafni, A.; Paz, Z.; Sztejnberg, A. A tale of three acaropathogenic fungi in Israel: *Hirsutella*, *Meira* and *Acaromyces*. *Exp. Appl. Acarol.* **2008**, *46*, 183–194. [CrossRef] [PubMed]

16. Paz, Z.; Burdman, S.; Gerson, U.; Sztejnberg, A. Antagonistic effects of the endophytic fungus *Meira geulakonigii* on the citrus rust mite *Phyllocoptruta oleivora*. *J. Appl. Microbiol.* **2007**, *103*, 2570–2579. [CrossRef]

17. Sztejnberg, A.; Paz, Z.; Boekhout, T.; Gafni, A.; Gerson, U. A new fungus with dual biocontrol capabilities: Reducing the numbers of phytophagous mites and powdery mildew disease damage. *Crop. Prot.* **2004**, *23*, 1125–1129. [CrossRef]

18. Paz, Z.; Gerson, U.; Sztejnberg, A. Assaying three new fungi against citrus mites in the laboratory, and a field trial. *Biocontrol* **2007**, *52*, 855–862. [CrossRef]

19. Cao, Y.; Li, P.-D.; Zhao, J.; Wang, H.-K.; Jeewon, R.; Bhoyroo, V.; Aruna, B.; Lin, F.-C.; Wang, Q. Morph-molecular characterization of *Meira nicotianae* sp. nov., a novel basidiomycetous, anamorphic yeast-like fungus associated with growth improvement in tobacco plant. *Phytotaxa* **2018**, *365*, 169–181. [CrossRef]

20. Han, X.; Li, P.; Luo, X.; Qiao, D.; Tang, X.; Li, G. Two new compounds from the marine sponge derived fungus *Penicillium chrysogenum*. *Nat. Prod. Res.* **2020**, *34*, 2926–2930. [CrossRef]

21. Dos Santos, A.; Rodrigues-Filho, E. New $\Delta^{8,9}$-pregnene steroids isolated from the extremophile fungus *Exophiala oligosperma*. *Nat. Prod. Res.* **2021**, *35*, 2598–2601. [CrossRef]

22. Shalit, Z.A.; Valdes, L.C.; Kim, W.S.; Micalizio, G.C. From an ent-Estrane, through a nat-Androstane, to the Total Synthesis of the Marine-Derived $\Delta^{8,9}$-Pregnene (+)-03219A. *Org. Lett.* **2021**, *23*, 2248–2252. [CrossRef]

23. Zhang, Y.; Zhou, X.; Huang, H.; Tian, X.; Song, Y.; Zhang, S.; Ju, J. 03219A, a new $\Delta^{8,9}$-pregnene isolated from *Streptomyces* sp. SCSIO 03219 obtained from a South China Sea sediment. *J. Antibiot.* **2013**, *66*, 327–331. [CrossRef]

24. Qiu, S.X.; van Hung, N.; Xuan, L.T.; Gu, J.Q.; Lobkovsky, E.; Khanh, T.C.; Soejarto, D.D.; Clardy, J.; Pezzuto, J.M.; Dong, Y.M.; et al. A pregnane steroid from Aglaia lawii and structure confirmation of cabraleadiol monoacetate by X-ray crystallography. *Phytochemistry* **2001**, *56*, 775–780. [CrossRef]

25. Cao, V.A.; Kwon, J.H.; Kang, J.S.; Lee, H.S.; Heo, C.S.; Shin, H.J. Aspersterols A-D, Ergostane-Type Sterols with an Unusual Unsaturated Side Chain from the Deep-Sea-Derived Fungus *Aspergillus unguis*. *J. Nat. Prod.* **2022**, *85*, 2177–2183. [CrossRef] [PubMed]

26. Demarco, P.V.; Farkas, E.; Doddrell, D.; Mylari, B.L.; Wenkert, E. Pyridine-induced solvent shifts in the nuclear magnetic resonance spectra of hydroxylic compounds. *J. Am. Chem. Soc.* **1968**, *90*, 5480–5486. [CrossRef]

27. Luo, X.; Li, F.; Shinde, P.B.; Hong, J.; Lee, C.O.; Im, K.S.; Jung, J.H. 26,27-cyclosterols and other polyoxygenated sterols from a marine sponge *Topsentia* sp. *J. Nat. Prod.* **2006**, *69*, 1760–1768. [CrossRef] [PubMed]

28. Shi, Q.; Huang, Y.; Su, H.; Gao, Y.; Peng, X.; Zhou, L.; Li, X.; Qiu, M. C_{28} steroids from the fruiting bodies of *Ganoderma resinaceum* with potential anti-inflammatory activity. *Phytochemistry* **2019**, *168*, 112109. [CrossRef] [PubMed]

29. Han, Y.; Cheng, Y.; Tian, L.W. Semisynthesis of 22,25-Epoxylanostane Triterpenoids: Structure Revision and Protective Effects against Oxygen-Glucose Deprivation/Reoxygenation Injury in H9c2 Cells. *J. Nat. Prod.* **2023**, *86*, 406–415. [CrossRef] [PubMed]

30. Lee, H.S.; Kang, J.S.; Cho, D.Y.; Choi, D.K.; Shin, H.J. Isolation, Structure Determination, and Semisynthesis of Diphenazine Compounds from a Deep-Sea-Derived Strain of the Fungus *Cystobasidium laryngis* and Their Biological Activities. *J. Nat. Prod.* **2022**, *85*, 857–865. [CrossRef]

31. Li, M.; Li, S.; Hu, J.; Gao, X.; Wang, Y.; Liu, Z.; Zhang, W. Thioester-Containing Benzoate Derivatives with alpha-Glucosidase Inhibitory Activity from the Deep-Sea-Derived Fungus *Talaromyces indigoticus* FS688. *Mar. Drugs* **2021**, *20*, 33. [CrossRef] [PubMed]

32. Zhao, W.; Zeng, Y.; Chang, W.; Chen, H.; Wang, H.; Dai, H.; Lv, F. Potential α-Glucosidase Inhibitors from the Deep-Sea Sediment-Derived Fungus *Aspergillus insulicola*. *Mar. Drugs* **2023**, *21*, 157. [CrossRef] [PubMed]